EESTI NSV TEADUSTE AKADEEMIA TOIMETISED. 22. KÖIDE
FÜÜSIKA * MATEMAATIKA. 1973, NR. 1

ИЗВЕСТИЯ АКАДЕМИИ НАУК ЭСТОНСКОЙ ССР. ТОМ 22
ФИЗИКА * МАТЕМАТИКА. 1973, № 1

https://doi.org/10.3176/phys.math.1973.1.07

УДК 539.28

*A. SÜGIS, M. ALLA*

# INSTABILITY INVESTIGATION OF NMDR SPECTROMETERS

## Introduction

The degree of stabilization of the ratio of magnetic field to radio-frequency is one of the most important parameters in high resolution NMR spectrometers. In the case of monoresonance or double resonance with weak perturbing rad ofrequency field $H_2$ (spin-tickling) maximum stability is required in time domain from tenths of seconds towards longer times while in experiments with strong $H_2$ (nuclear Overhauser effect, collapse, INDOR) maximum stability is essential even in the millisecond range. Strong $H_2$ influences the NMR line to be observed via noise sideband produced by spectral components of fluctuations of field-frequency ratio near the frequency difference of observing radio-frequency field $H_1$ and $H_2$ and gives excess noise output at the frequency of NMR line to be observed. Such disturbance will diminish the accuracy of measurements in NMDR spectra.

Instability can be described in frequency domain by the mean-square spectral density $S_y(f)$ of the instantaneous fractional perturbations $y(t)$ of field-frequency ratio, where $f$ is Fourier frequency and $S_y(f)$ [$\mathrm{Hz}^{-1}$] is meant one-sided [1]. However, further we use $R(f)$, the square root of $S_y(f)$, as more closely related to experiments ($R^2(f) = S_y(f)$).

## Instability factors and characterization

First we consider instability arising from the thermal noise of the stabilizer's probe circuit that is the governing factor of stabilizer's instability. Other factors, such as phase drift and fluctuations or excess noises in an amplifier, can be kept well below and this is really the case in up-to-date designs. In stabilizer loop this thermal noise acts as internal additive noise [2], giving white noise frequency modulation of stabilizer's radiofrequency signal [3,4], i. e. $R'_1(f) = \mathrm{const}$. The same noise source contributes to the output (control) voltage as well, and then it acts as external additive noise, giving white noise phase modulation, i. e. $R''_1(f) = f \times \mathrm{const}$.

In order to get an expression for instability arising from stabilizer itself, we should add $R'_1(f)$ and $R''_1(f)$ linearly rather than in quadrature: $R_1(f) = R'_1(f) + R''_1(f)$, since both instability components are fully correlated due to the same noise source. Then

$$R_1(f) = \frac{2}{\nu_0 Q_s}\left(\frac{1}{2\pi T^*_{2s}} + f\right), \qquad (1)$$

where $\nu_0$ is the Larmor frequency, $1/\pi T_2^*$ designates instrumental linewidth of stabilizer's sample, and $\varrho_s = V_s/V_n$ is signal-to-noise ratio with peak value of stabilizer's radiofrequency signal $V_s$ and rms noise voltage per 1 Hz $V_n$. Uncorrelated noise contributions from both sidebands are accounted in Eq. (1). Somewhat analogous expressions have been published for a feedback oscillator [5] or a maser [6], but for uncorrelated noise sources.

Schematic plots of $R_1(f)$ along with other instability factors are given in a log-log scale in Fig. 1. The total magnetic field instability is represented by Curve $R_0(f)$, and $R_2(f)$ is the differential field instability between stabilizing and analytical samples. Residual instability of a spectrometer $R_r(f)$ contains the whole amount of $R_1(f)$ and $R_2(f)$ within spin stabilizer's passband, while out of this range $R_r(f)$ is determined by $R_0(f)$. The appropriate expression is:

$$R_r^2(f) = (R_1^2(f) + R_2^2(f))\, W^2(f) + R_0^2(f)/K^2(f), \qquad (2)$$

where $K(f) \equiv |K(2\pi if)|$ is stabilization coefficient of a spin stabilizer and $W(f) \equiv |W(2\pi if)|$ is its transfer function while well-krown relation between them reads $K(2\pi if) = 1/(1 - W(2\pi if))$. A corresponding pair of $K(f)$ and $W(f)$ is plotted (in the same log scale) in Fig. 1 along with the Curve $R_r(f)$ according to Eq. (2).

Now it should be obvious how important is the particular shape of stabilizer's frequency response and peaking of this response ($W(f) > 1$, $K(f) < 1$) is a harmful quality since it leads to amplification of noise from all sources.

Time-domain ("short-term") characterization of instability can best be obtained by using average value of sample variance $\langle \sigma_y^2(N, T, \tau) \rangle$ with $N = 2$, $T = \tau$, denoting it by $\sigma_y^2(\tau)$ [1]. This is a good way to do away with nonconvergence of $\langle \sigma_y^2(N, T, \tau) \rangle$ with increasing $N$, especially for the case of "flicker noise" frequency modulation [3] — as it is just the case for $R_2(f)$ at lower $f$. The expression

$$\sigma_y^2(\tau) = 2 \int_0^\infty R_r^2(f) \left( \frac{\sin^2 \pi f\tau}{(\pi f\tau)^2} - \frac{\sin^2 2\pi f\tau}{(2\pi f\tau)^2} \right) df \qquad (3)$$

gives a measure of instability over an observation interval $\tau$ [1], where a suitable weighing function (in parentheses) emphasizes the part of spectrum around $f \approx 1/3\tau$.

## Measurement and evaluation

The instrumentation used for instability measurements consisted of a 40-MHz special proton spectrometer system shown in Fig. 2 and JEOL electromagnet JM-300 with flux stabilizer JNS-H. This system enables to perform measurements in the Fourier frequency range $f = 0.01 \ldots 1000$ Hz using external as well as internal locks. It proved to be essential to use another nucleus for internal lock due to unavoidable although small interference between measuring and control channels.

The simplest algorithms were used for frequency conversion to obtain maximal spectral purity. Frequency synthesizers (II, III) are based on algorithm $39{,}450 + (550 + f_s)$, where 39,445 kHz is quartz stabilized, 550 kHz is obtained from a stable varactor-controlled LC-oscillator in an automatic phase control loop with $f_s = 5 \ldots 7$ kHz from shift or sweep

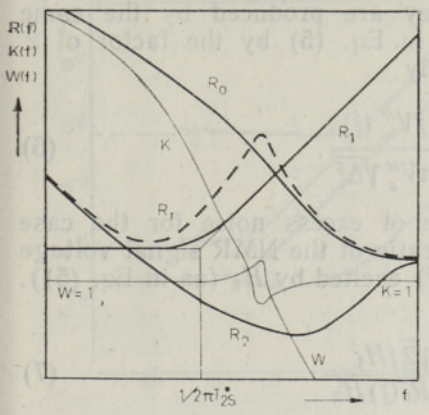


Fig. 1

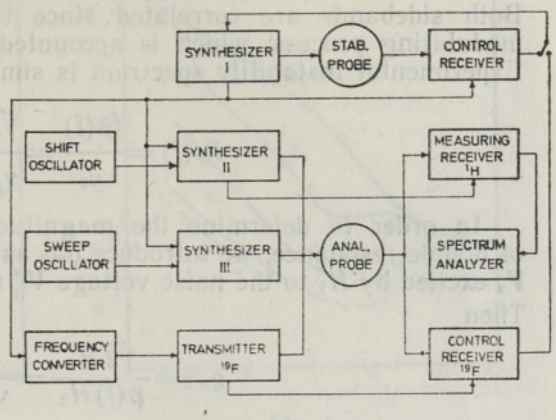


Fig. 2

oscillators. Spin stabilizer controls the 550-kHz oscillator in Synthesizer I directly. The frequency converter $^1H/^{19}F$ takes 40,000 kHz from Synthesizer I and consecutively divides it by 5; 2; 2; 2; 2; 2, and 2 followed by three consecutive adding procedures: $125 + 250 = 375$ kHz; $2{,}000 + 375 = 2{,}375$ kHz, and $40{,}000 - 2{,}375 = 37{,}625$ kHz. Residual frequency difference (about 6.7 kHz) is covered by field modulation.

The lower part of spectrum ($f = 0.01 \ldots 40$ Hz) was measured by centering Synthesizer II on a dispersion line and recording the rms noise voltage $V_n'(f)$ at the output of the spectrum analyzer which had constant fractional bandwidth $\Delta f/f = 0.2$. Calibration was obtained by measuring the central slope $C_m$ [V/Hz] and instrumental linewidth $1/\pi T^*_{2m}$ of the measuring NMR line. Experimental instability spectrum can now be calculated from the following:

$$R_r(f) = \frac{V'_n}{v_0 C_m \sqrt{\Delta f}} (1 + 2\pi T^*_{2m} f), \tag{4}$$

where $\Delta f$ is spectrum analyzer's bandwidth and $2\pi T^*_{2m} f$ takes into account filtering action of the measuring line for frequencies out of its bandwidth.

For the measurement of the upper part of spectrum ($f = 20 \ldots 1000$ Hz) the whole spectrometer was acting as an instability ("noise sideband") spectrum analyzer.

Synthesizer II was centered on a single absorption line and then its output (field $H_1$) was switched off. Nevertheless, it remains to supply reference voltage at the frequency of the measuring line to the receiver. Subsequently output of Synthesizer III (field $\gamma H_2/2\pi$ up to 10 Hz) was switched on and its frequency scanned, while spectrum analyzer itself was permanently in 1-Hz position. Now the rms noise voltage $V''_n(f)$ at the output of the spectrum analyzer is a measure of instability at the Fourier frequency, equalling the frequency difference between Synthesizers II and III. For calibration, field $H_2$ was reduced $n$ times and the frequency difference between Synthesizers II and III set to a very low value, say 0.1 Hz. Resulting beatnote with rms value $V''_s$ is a measure of NMR signal. The rms noise modulation index becomes then

$$\beta(f) = 2V''_n(f)/nV''_s\sqrt{2\Delta f}. \tag{5}$$

Both sidebands are correlated since they are produced by the same modulating process, which is accounted in Eq. (5) by the factor of 2. Experimental instability spectrum is simply

$$R_r(f)=\frac{f\beta(f)}{\nu_0}=\frac{\sqrt{2}\,fV''_n(f)}{\nu_0 nV''_s\sqrt{\Delta f}}. \tag{6}$$

In order to determine the magnitude of excess noise for the case of double resonance, we introduce $\varrho_{m2}$ as ratio of the NMR signal voltage $V_s$ excited by $H_1$ to the noise voltage $V''_n(f)$ excited by $H_2$ (as in Eq. (5)). Then

$$\varrho_{m2}=\frac{\sqrt{2}\,H_1}{\beta(f)H_2}=\frac{\sqrt{2}\,fH_1}{\nu_0 R_0(f)H_2} \tag{7}$$

or within stabilizer's bandwidth

$$\varrho_{m2}=\frac{\varrho_s H_1}{\sqrt{2}\,H_2}. \tag{8}$$

Sample substance for separate probes was water with admixtured paramagnetic ions to obtain suitable linewidths: 25...40 Hz for external lock and 3...30 Hz for measuring sample. For common probe a 50/50 v. v. mixture of $C_6H_6$ and $C_6F_6$ was used, while linewidths from 0.5 up to 14/7 Hz ($^1H/^{19}F$) were obtained with dissolved ferric acetylacetonate.

## Results and discussion

Separation of stabilizer's instabilities $R_1(f)$ and $R_2(f)$ from total field instability $R_0(f)$ (see Eq. (2)) was obtained by the use of maximally fast frequency regulation [7]. Further, separate measurement of $R_1(f)$ and $R_2(f)$ is not possible in the whole frequency range, but by variation of $\varrho_s$ as well as configurations of probes (external or internal lock, distance of probes) rather clear results were obtained.

Some characteristic cases for $R_1(f)$ are presented in Fig. 3, where solid curves represent experimental results and dashed curves are calculated from Eq. (1). Curves *1* and *2* correspond to the same signal-to-noise ratio $\varrho_s=110$ while differing in linewidth: $1/\pi T^*_{2s}$ is equal to 32 and 0.6 Hz, respectively. Curves *3* and *4* have $\varrho_s$'s 450 and 28,000 and linewidths, on the contrary, 0.6 and 32 Hz. Breaking point at half-linewidth is sufficiently marked, and even a feeble upward slope of experimental curves towards lower frequencies can probably be assigned with refinements of theory of oscillators (see [2], Sec. III A. 2).

The instability component $R_1(f)$ is quite a well-defined quantity, but the following components (Fig. 4) are purely experimental and depend on the magnet system used, environmental conditions, etc. And yet, some characteristic dependences can be established. Total field noise of a JM-300 electromagnet with JVR-3 regulator in average environmental conditions is presented by Curve $R_0(f)$. Stabilizing action of a flux stabilizer JNS-H is indicated by Curve $R_0'(f)$. Detailed investigation [8] has shown that performance of a flux stabilizer depends critically not on its amplifier but on configuration and location of its coils and is due to the inherent flux-field error. At the same time instability level $R_0'(f)$ is not only due to insufficient effective gain of a flux stabilizer (according to measured flux-field error) but is also caused by a component of field

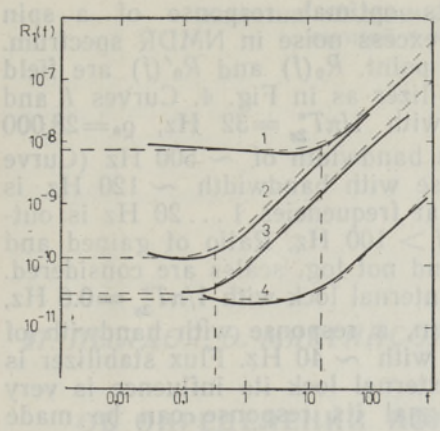


Fig. 3

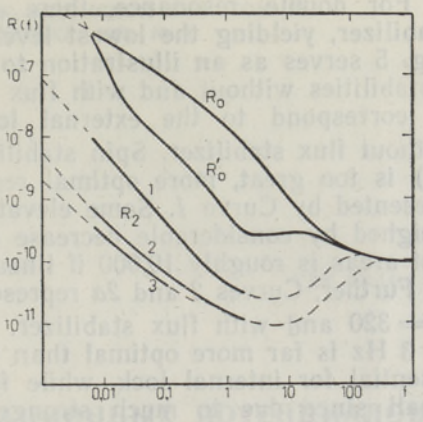


Fig. 4

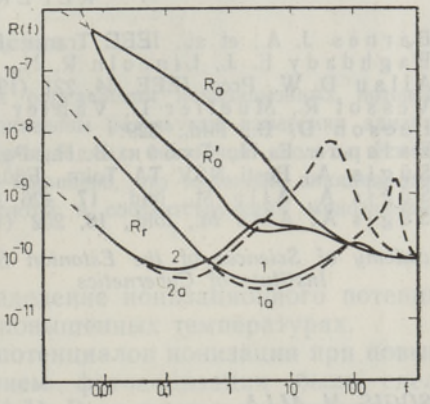


Fig. 5

instability in the air gap center that is independent of flux instability. Such instability caused by field redistribution is of the same origin as differential instability $R_2(f)$ to be discussed next.

Differential instability $R_2(f)$ for external stabilizer with a distance of 22 mm between centers of probes is represented by Curve *1*. This instability component is quite independent of total field instability, and no improvement was noticed when flux stabilizer was switched on, yielding lower level $R_0'(f)$ instead of $R_0(f)$. Curve *2* represents diminished differential instability for a special probe head with an annular stabilizer sample surrounding measuring probe [9]. These samples have complete radiofrequency shielding between them yielding independent channels. Inner and outer diameters of stabilizer sample are 10/17 mm. Measurement of $R_2(f)$ for Curves *1* and *2* above 2 Hz is hindered by component $R_1(f)$ (in spite of the rather high $\varrho_s = 100{,}000$ for annular sample). However, the shape of Curves *1* and *2* (dashed portion between 2 ... ... 200 Hz) was deduced from differential perturbation measurements [8].

An internal $^{19}F$ stabilizer gave an unexpectedly high level of "differential" instability (Curve *3*) as compared to the external stabilizer, although all possible instrumental noise sources were carefully eliminated, including quartz control of all audiofrequencies. This instability level has been measured for the spinning sample with instrumental linewidth for both lines equalling 0.6 Hz and gives variance $\sigma_{y(\tau=10)} = 2.4 \times 10^{-11}$ (about 1 mHz) over 10-sec observation interval, which was calculated from Eq. (3) as well as measured in the same conditions as Curve *3*. This instability can probably be assigned to fluctuations in line shape while there exist slighly different conditions in two channels: radiofrequency power, linewidths and operating points on the lines are not identical. Doubtlessly, considerably lower level of such instability can be observed in modern magnets having better resolution stability.

For double resonance, there exists optimal response of a spin stabilizer, yielding the lowest level of excess noise in NMDR spectrum. Fig. 5 serves as an illustration to the point. $R_0(f)$ and $R_0'(f)$ are field instabilities without and with flux stabilizer as in Fig. 4. Curves *1* and *1a* correspond to the external lock with $1/\pi T_{2s}^* = 32$ Hz, $Q_s = 28{,}000$ without flux stabilizer. Spin stabilizer's bandwidth of $\sim 500$ Hz (Curve *1a*) is too great, more optimal response with bandwidth $\sim 120$ Hz is presented by Curve *1*. Some elevation at frequencies 1 ... 20 Hz is outweighed by considerable decrease for $f > 100$ Hz. Ratio of gained and lost areas is roughly 10,000 if linear, and not log, scales are considered.

Further, Curves *2* and *2a* represent internal lock with $1/\pi T_{2s}^* = 0.6$ Hz, $Q_s = 320$ and with flux stabilizer. Again, a response with bandwith of $\sim 3$ Hz is far more optimal than that with $\sim 40$ Hz. Flux stabilizer is essential for internal lock, while for external lock its influence is very small since due to much stronger signal its response can be made accordingly faster.

## REFERENCES

1. Barnes J. A., et al., IEEE Trans., IM-20, 105 (1971).
2. Baghdady E. J., Lincoln R. N., Nelin B. D., Proc. IEEE, 53, 704 (1965).
3. Allan D. W., Proc. IEEE, 54, 221 (1966).
4. Vessot R., Mueller L., Vanier J., ibid., 199.
5. Leeson D. B., ibid., 329.
6. Базаров Е. Н., Губин В. П., Радиотехника и электроника, 15, 2134 (1970).
7. Sügis A., Eesti NSV TA Toim., Füüs. Matem., 18, 304 (1969).
8. Sügis A., Alla M., ibid., 17, 426 (1968).
9. Sügis A., Alla M., ibid., 18, 252 (1969).

*Academy of Sciences of the Estonian SSR,*
*Institute of Cybernetics*

Received
Sept. 6, 1972

*A. SÜGIS, M. ALLA*

**TMTR-SPEKTROMEETRITE EBASTABIILSUSE UURIMINE**

*А. СЮГИС, М. АЛЛА*

**ИССЛЕДОВАНИЕ НЕСТАБИЛЬНОСТИ ЯМДР-СПЕКТРОМЕТРОВ**

Измерена спектральная плотность нестабильности отношения напряженности магнитного поля к частоте ВЧ-поля для ЯМР-спектрометра высокого разрешения в диапазоне от 0,01 до 1000 *гц* при различных спиновых стабилизаторах. Рассмотрено влияние ширины ЯМР-линии и быстродействия как внутреннего, так и внешнего спинового стабилизаторов на стабильность спектрометров. Для гомоядерного двойного резонанса с сильным возмущающим полем спектральные компоненты нестабильности довольно высокой частоты (10—200 *гц*) являются существенными. Описываются методы и аппаратура измерения.